Insight into the Geothermal Structure in Tatun Volcano Group, Taiwan

Chi-Hsuan Chen[1], Po-Tsun Lee[1], Chang-Cheng Lin[1], Lun-Tao Tong[2], Tai-Rong Guo[2], Wayne Lin[2] and Mien-Ming Chen[1]

[1]Central Geological Survey, MOEA, New Taipei City, Taiwan.

[2] Industrial Technology Research Institute, Hsinchu County, Taiwan.

prochen@moeacgs.gov.tw

aiwalee@moeacgs.gov.tw

Keywords: *Geothermal Structure, Tatun Volcanic Group, 3D Inversion, Database, Conceptual Model.*

ABSTRACT

The Tatun Volcano Group (TVG) which is known as the highest temperature geothermal field in Taiwan. There are four geothermal potential areas named Beitou, Matsao, Shi-Huang-Ping and Chinshan. The government conducted exploration activities in the late 1960s focused on these areas. The highest drilling temperature encountered, nearly 290 ℃ at the Matsao area at a depth of less than 2 km, implies there is a commercial temperature for power generation. However, the geothermal development has been suspended due to a high acid content and highly corrosive fluids. Last decade, some review and exploration activities raised the possibility of finding neutral brine and developing geothermal generation at TVG. This study integrates previous research studies and newly completed geological, geophysical and geochemical surveys to establish a geothermal conceptual model of the TVG. The deep hydrothermal fluid along the extensional fracture is one of the primary heat sources in TVG that meets the criteria of high temperature and neutral geothermal brine based on E208 drilling data. Based on the MT 3D resistivity model, a total of 5 low resistivity areas that could be the possible clay cap are proposed. The low-resistivity is located at the bottom of the volcanic rock body, and the resistivity, as low as 10 ohm-m, is consistent with the mineral character of smectite, illite, and chlorite. All the data mentioned above was transformed into digital form and combined with the TWD97 projection system. Finally, a digital 3D geothermal conceptual model based on Leapfrog geothermal was established.

There are some areas with high temperature and low acid fluid in the TVG area, from the perspective of the geochemistry view. However, the new proposed potential areas need further confirmation by the drilling of an exploration well.

Applying developed volcanic activity observation techniques to monitor environmental changes while conducting geothermal surveys can ensure the safety of future geothermal development efforts.

1. OVERVIEW

1.1 Geological settings

The TVG is located at the southwest end of the rift zone along the southern Taiwan-Sinzi Folded Zone. The Oligocene/Miocene sedimentary rocks were affected by the arc-continent collision and pushed along the detachment structure to the current Tatun volcanic area (Hsiao *et al.*, 1998). As the subduction of the plate gradually proceeded and the collision gradually slowed, the Tatun volcanic area resumed the fractured terrain structural model again, and the magma moved upward along the fractured structural belts in the directions of NE (~N56°E) and NEE (N68°E–N85°E). The magma penetrates the detachment structure, intrudes into the sedimentary rock base to form igneous rock intrusions, and even erupts to the surface to form the TVG.

In the later stage of the volcanic eruption, due to the change of the earth's stress field and the collapse of the volcanic body, several normal fault structures in the direction of NNE and NNW were formed, cutting through the Tatun volcanic rock mass. The deep magma-derived hydrothermal fluids migrate upward along the aforementioned NE and NEE-directed tensile fracture structures that cut through the deep part of the crust, and form a geothermal structural system. The later NNE and NNW structures that cut through the volcanic body, are mainly distributed between the Shanchiao fault and the Kanchiao fault (Lee and Wang, 1988; Teng, 1996).

1.2 History of geothermal survey

In the 1960s, Taiwan was in the period of long-term economic re-construction after World War II, and its demand for energy was extremely urgent. Due to the active volcanic activity and hot spring resources in the TVG, at the suggestion of the US military advisory group, the geothermal survey of the Tatun volcanic area began to be planned in Taiwan. The earliest geothermal survey work began in 1966. The survey projects included a geological survey, surface temperature measurement, hot spring sampling and analysis, a geophysical survey, exploration well drilling, steam flow and heat enthalpy measurement, etc. The survey work at this stage ended in 1972. The total exploration area was about 200 square kilometers, and 82 wells were drilled with a total length of 21,188 meters, including two exploration wells with a depth of 1,500 meters. In the TVG area, the highest underground temperature of 293 ℃ is located in the Matsao area (well E208). The highest temperature area is a layer of mid to coarse sandstone with good permeability. At the same time, the Matsao area also has good geothermal conditions for the presence of shallow clay caps. Based on the average evaluation of the results of various investigations, the shallow geothermal potential of the geothermal reservoir in the TVG is 85MWe. If the deep geothermal resource is included in the calculation, the geothermal potential could be greater than 500MWe (Lee *et al.*, 1994).

Although there is a considerable potential for geothermal storage, the underground fluid in the Tatun volcanic area is acidic, rich in chloride ions, sulfate radicals and ammonium radicals that are corrosive to metals. Not only is the fluid highly corrosive to machinery and equipment, but subsequent geothermal development, plant construction and operation will require more investment, and it also poses a

ISSN 2703-4275

great threat to the safety of operators. Therefore, as is mentioned in the conclusion of the geothermal survey results for the TVG, it is necessary to first solve the problem of acid corrosion, before setting up the test power plant.

After obtaining the survey results for the TVG, in 1973, and with the arrival of the first oil crisis, Taiwan's geothermal survey work considered other non-volcanic geothermal areas, but continued to focus on the acid corrosion resistance of pipes. However, in 1985, part of the Great Volcano Group was included in the newly established Yangmingshan National Park, which includes most of the geothermal areas such as Matsao, Dayoukeng, Siaoyoukeng and Liuhuangu. Under the regulations of the National Park decree, geothermal development work in these areas was temporarily suspended.

1.3 Volcanic Activities

The volcanic activities of the TVG began 2.4 to 2.8 million years ago and it has experienced several large-scale eruptions so far (Song and Lo, 1995). A uranium-thorium-radium dating of andesite extruded from the area shows that the most recent eruption was about 1,370 years ago (Zellmer *et al.*, 2015). In addition to the very young age of the volcanic eruption, there are still many volcanic and geothermal activities in the TVG, such as hot springs, and micro-earthquakes. This means that there is still a source of high heat flow and gas deep in the crust. In volcanic geothermal areas, a high-temperature magma heated reservoir is a natural consequence.

There are two main scientific findings for inferring the presence of a magma reservoir. One is from the helium isotope ratio ($^3He/^4He$) in volcanic gas. The analysis and calculation of the composition of volcanic gases of the TVG shows that a high proportion (60-80%) of the helium isotope is released by magma, rather than corresponding to the helium isotope value in the general crust or air; especially in the Dayoukeng area most obviously, as its $^3He/^4He$ value (R_A) is 6 to 8 which is close to the helium isotope ratio of active volcanoes in neighboring countries such as Japan and the Philippines (Yang *et al.*, 1999).

Another piece of evidence comes from microseismic records; for a long time, there have been quite a few microseismic occurrences near the TVG, especially concentrated in Mt. ChiHsin, Dayoukeng and Bayan areas. Since 2003, a dense network of microseismic stations has been set up in the TVG to continuously record and analyze earthquake records. It was found that the waveform and frequency of these dense microseismic signals on the recorder have the same characteristics as the volcanic seismic signals in many active volcanic areas, such as swarms, long-period vibrations, tremors, etc. (Lin *et al.*, 2005). Since the Tatun volcanic area is close to the urban area of the capital, it is difficult to use ground-based artificial seismic sources. Scientists have observed the phenomenon of S-wave shadowing and P-wave slow arrival through the dense seismic station network, as well as the research results of the crustal velocity structure characteristics, confirming that there is a magma reservoir under the Tatun volcano (Lin, 2016). Its location is probably at the bottom of Dayoukeng and Mt. Huangzui. It is cylindrical, about 12 kilometers long and about 4 kilometers in radius (Huang *et al.*, 2021).

Since the TVG conforms to the definition of active volcanoes, the Taiwan government is currently conducting a number of observations of volcanic activity, and continues to upgrade volcano monitoring technology and equipment.

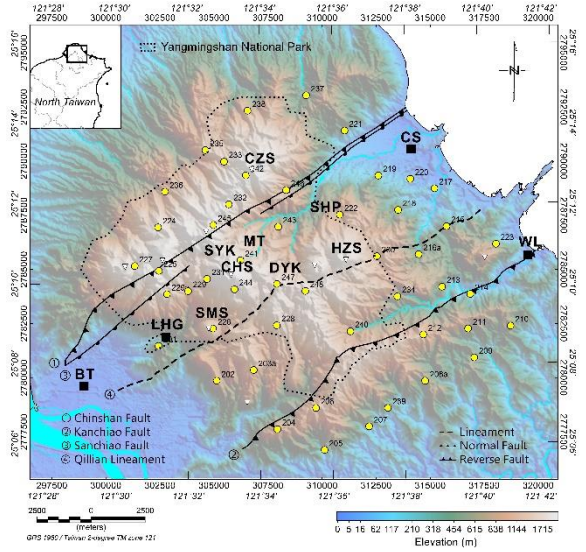

Figure 1: The coverage of MT stations (yellow spots) in the TVG discussed in this study. The abbreviation of the local names mentioned in the paper are as: Chinshan (CS), WanLi (WL), Shi-huang-ping (SHP), Matsao(MT), Liuhuangu (LHG), Dayoukeng(DYK), Siaoyoukeng (SYK). The names of mountains, Mt. Shamao (SMS), Mt. ChiHsin (CHS) and Mt. Huangzui (HZS).

2. ADVANCED EXAMINATION AND SURVEY

Previous studies have provided preliminary results on the potential magma chamber, volcanic fluid circulation, and post-volcanic signatures due to the presence of volcanic activity in the TVG. However, the subsurface distribution of the geothermal system remains ambiguous. To clarify the geometry of the possible cap layer, intrusive body, fluid chamber, and fluid pathway, various geophysical surveys were re-examined, and supplementary investigations were carried out. These included aeromagnetic data, Magnetotelluric (MT) surveys, gravity data, seismic data, and previous drilling data. The aim of these investigations was to gain a better understanding of the subsurface structure and characteristics of the geothermal system in the TVG.

2.1 Re-examination of the magnetic data

The magnetic properties of the TVG offer important evidence for understanding the volcanic and geothermal processes in the area. The TVG experienced volcanic activity from 3 Ma to 1.37 ka, with the most active period occurring between 0.7 Ma and 0.2 Ma. (Wang and Chen, 1990, Tsao, 1994, Chu *et al.*, 2018). LiDAR DEM analysis identified 51 volcanic cones in the TVG, and aeromagnetic surveys and gravity data helped identify the distribution of volcanic bodies and rock boundaries (Chen *et al.*, 2007). By using numerical deviation enhancement techniques, the rock geometry and contact structures could be delineated. The study also discusses the magnetic degaussing feature (Soengkono, 2016) resulting from high temperatures or chemical alteration. Demagnetization features indicate that potential geothermal areas mainly occur near LHG, MT-DYK-SHP, and east of HZS areas (Fig. 2). The degree of demagnetization can serve as an indicator of the main

ISSN 2703-4275

hydrothermal activities and areas with less impact. Additionally, the 3D inversion of the total magnetic intensity (Tong and Lin., 2013) revealed low magnetic susceptibility (SI) vacuums surrounded by relatively high SI andesite bodies. It is worth mentioning that microearthquakes mainly occur within the boundary of the low SI vacuums (Fig. 3). The analysis of total magnetic intensity, magnetic lineation, and demagnetization features can provide valuable insights into the subsurface distribution of andesitic magnetic bodies, the presence of hydrothermal fluid chambers, and the deep-cut contact relationship of andesitic magnetic bodies.

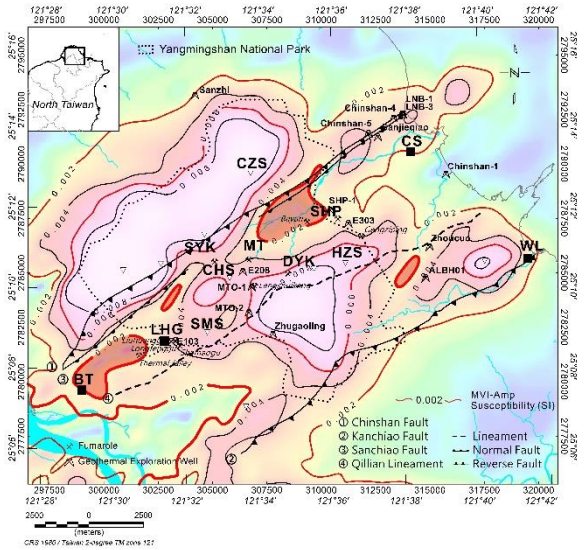

Figure 2: Magnetic susceptibility map of the TVG. The magnetic degaussing area, localized in three subareas, could be depicted with NE treading by the iso-values of SI.

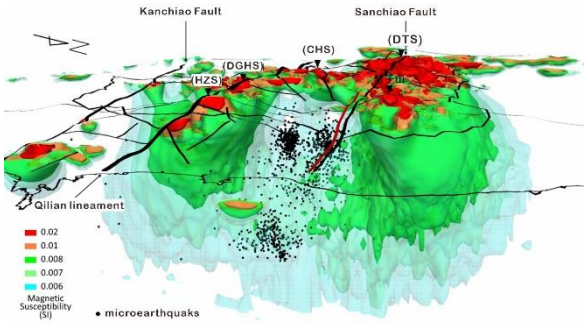

Figure 3: 3D view of microseismicity and magnetic susceptibility (SI) looking from NE to SW. The seismicity occurred between the area bounded by two faults and relative high SI bodies.

2.2 New MT (Magnetotelluric) Survey

The presence of a low-resistivity structure is closely associated with the smectite clay cap layer, suggesting an indirect indication of the high thermal gradient and low permeability of the cap. (Ussher *et al.*, 2000; Cumming, 2016). The shallow part of the cap layer consists of a near-neutral smectite or smectite-illite zone with resistivity less than 10 ohm-m, with a temperature in the range 100°C to 200°C. In the deeper part, where the temperature exceeds 200°C, the high resistivity core corresponds to a chlorite zone representing the fluid upwelling center. Therefore, an MT Survey is an important technique for exploring volcanic-type geothermal systems. In previous studies, more than 70 Audio-MagnetoTelluric (AMT) stations were deployed from 2013-2017 by Bureau of Energy, Ministry of Economic Affairs and Industry and Research Institute (Dobson *et al.*, 2018). However, due to the limitation in instrument bandwidth and 3D topography-related inversion techniques, the resistivity structures only revealed large-scale perturbations. To overcome this limitation, this study implemented a plan with wider station coverage and broadband MT instruments (MTU-5C, Phoenix Co.). Additionally, remote-reference processing was controlled to improve the data quality. Results from a total of 49 stations, each with a recording period of over 40 hours, were compiled for joint 3D inversion (Fig. 4). According to the recordings, the sounding curves (apparent resistivity vs frequency) characteristic could be described as follows:

- The resistivity characteristics of the volcanic geothermal field can be described as an H type (high-low-high) distribution toward the depth. In the high frequency band, high-resistivity are observed, which reflect the presence of surface volcanic rock. The low resistivity part of the curve may correspond to the alteration layer, indicating the presence of altered minerals.

- It is important to note that not all stations recorded the same frequency band due to unequal signal-to-noise ratio. Only 8 stations recorded data up to 0.01 Hz, while half of the recordings reached up to 0.35 Hz. After removing recordings of poor quality, a total of 43 stations were used for the 3D inversion.

The ModEM software (Egbert and Kelbert, 2012; Kelbert *et al.*, 2014) was utilized for the MT 3D inversion. To account for the effect of topography, a 200 m resolution topography was introduced for the surface grid boundary. The grid spacing is 250 m horizontally, with an unequal spacing interval from 15 m in the upper part to gradually increasing intervals of 15 m times 1.08, 1.15 and so on, in the deeper part, reaching the lowest boundary at 471 km. A forward modelling procedure was initially conducted to check the grid size. After 173 iterations, the root mean square value reduced from 11.42 to 1.62, indicating convergence in the inversion process. Based on the inverted resistivity model, a total of 5 low resistivity areas were identified (Fig 5). The low-resistivity layers were found to be located in the middle and bottom parts of the volcanic rock body and sedimentary layers, with a resistivity value below 10 ohm-m. In the sedimentary formation, areas with resistivity below 10 ohm-m are considered as andesite rock bodies by comparing with the inversion results of magnetic and gravity data. It is speculated that these low-resistivity areas smaller than 2 ohm-m (noted as C1-C5 in Fig. 5, Fig. 7) may be related to high-temperature fluids or alteration cap layers. The newly derived MT model provides important contraints on the potential geothermal areas (Tong *et al.*, 2020). We infer that the areas of low resistivity are due to low temperature alteration by neutral pH fluids and perhaps also smectite-rich sediments.

ISSN 2703-4275

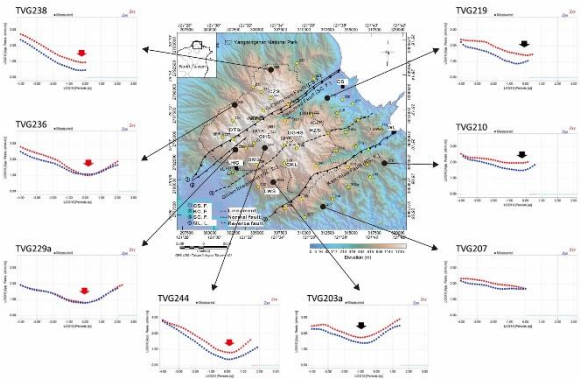

Figure 4: The measured sounding curve of the MT stations, which have been calibrated by remote reference processing. The arrows indicated the frequency band of low resistivity.

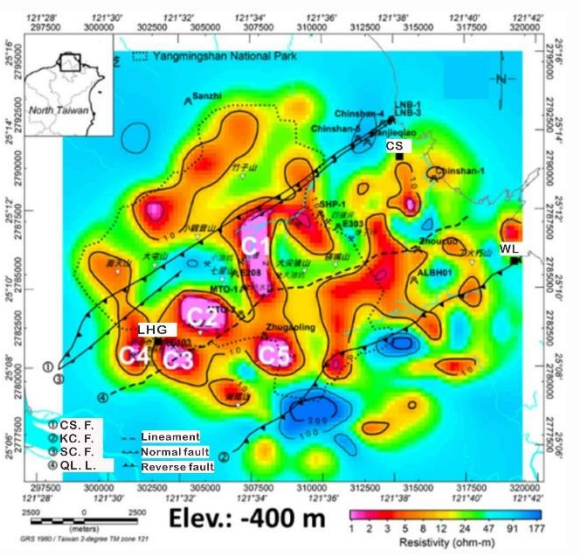

Figure 5: Resistivity slice at -400 m below sea level extracted from the 3d resistivity model. Five main geothermal systems (C1-C5) with low resistivity were depicted as the speculated geothermal systems.

2.3 Fracture System and Seismic Data

The fracture system plays a crucial role in the migration of geothermal fluid. However, identifying subsurface fractures or brittle faults can be challenging. Although thrust faults occurred in the Miocene sedimentary formation before the Tatun Volcano eruption, the Sanchiao normal fault reactivated along the thrust trace around 0.4 million years ago, indicating that the area is currently experiencing tensile stress (Teng *et al*., 2001). The use of 1m-resolution LiDAR DEM imagery allows for the delineation of the distribution of the topographic lineaments, which are related to rock cracks, as well as the orientation of fracture and fault planes (Yeh *et al*., 2014). By considering the stress environment, it is possible to advance the understanding of the reactivity potential of these fractures. The areas with the highest reactivity potential, as reveal by the analysis, are the SHP and CHS areas. These areas indicate the most likely domains for the presence of geothermal fluids (Tong *et al*., 2020).

In order to identify the possible deep-cut structures in the volcanic geothermal field, the analysis of large-scale magnetic structures can be helpful. Various numerical methods, such as vertical derivative, total horizontal derivative, tilt derivative, and analytic signal methodology are useful. Based on the magnetic characteristics, 17 distinct discontinuities (m1-m17 in the Fig. 6) have been identified. The lineation direction is predominantly in the NNE direction, with some segments in the NNW direction. Additionally, the seismicity groups in the area are found to be located at different depths beneath the CHS, DYK, and CKL area. Although these earthquakes are identified as important evidence for an active volcano in CHS (Lin, 2005; Pu *et al*., 2020a) they may be the result of gas or fluid activities in a narrow conduit beneath DYK (Pu *et al*., 2020b). They appear to be divided into different groups based on possible structures. The hydrothermal layer was identified by an inflation source of seismicity character at depth of 0.7 km and 2 km (Lin *et al*., 2019; Pu *et al*., 2020). These finding confirm the activities of geothermal gas and fluid that could be ascending along the pathway.

In the study area, the elevated temperature profile in NE-SW direction suggests the presence of at least three main geothermal fluid up-flow systems. These systems are thought to be located beneath the SMS, CHS, and SHP. By comparing the resistivity model, seismicity patterns, and the subvertical extension of the magnetic lineaments, it is possible to isolate discrete sub-systems associated with geothermal fluid activities (Fig 7).

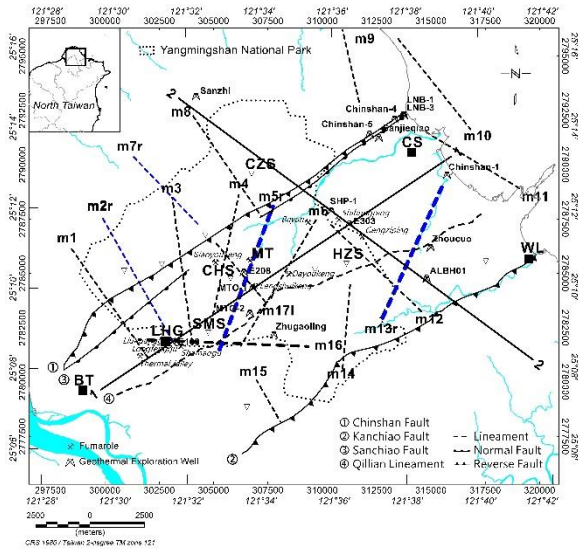

Figure 6: The NNE and NNW magnetic discontinuous boundaries (m1~m17) oblique contact with the NE fault system.

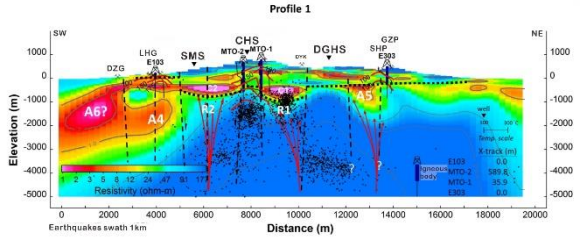

Figure 7: The NE trending resistivity profile are taken as the important base map for phenomena

ISSN 2703-4275

discussion. The subvertical dash lines represent the possible structures. Temperature contours (red lines) and lithology boundary (black dots) depicted according to the drilling data. Seismicity denoted as black point clusters. Accordingly, red lines with arrow suggest the upwell pathway of geothermal fluids.

2.4 Drilling Data

The volcano eruptions in the study area occurred within the Tertiary sedimentary layer, and the tensile tectonic environment cause the sediment basement to collapse in a concave shape. In order to construct a conceptual model of geothermal fluid circulation, it is important to consider the boundary between the sedimentary and volcanic rock layers. The presence of a dike or volcanic body intrusion in the sediment layer has been discussed in a previous study based on drilling cutting and cores, which is important for identifying the acid water-rock reactions (Rae *et al*., 2019). This study compiled reports from over 90 drilling data, with lithology logging available for 40 of them. Among these wells, 13 coincide with sedimentary basement at the deeper part.

To aid in the identification of boundaries, a 3D resistivity model was adopted. The drilling records of wells E208, SHP-1, and Chinshan-1, indicates the presence of a thick intrusive igneous rock within the sedimentary formation (Fig 8). These findings are supported by aeromagnetic and gravity data, as well as the altered minerals in the boreholes. The scale of the intrusion is important for understanding the potential heat source and the neutralization capacity of the geothermal system.

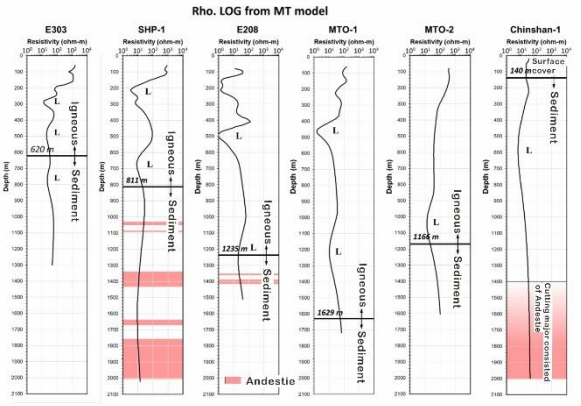

Figure 8: Lithological logs of drilling data in the TVG area. The resistivity columns extracted from the resistivity model are taken for the reference of lithology changes. Part of recordings reveal the intrusion occurs at the deep part in the sediment layer.

3. DATA MANAGEMENT AND DISCUSSION

3.1 Revised conceptual model

To complete the conceptual model, additional geophysical and geochemical evidence from other studies needs to be incorporated. A new model from a 3D joint seismic tomography inversion has revealed a magmatic heat source, indicated by a notable P-wave velocity reduction, located between 8 km to 20 km beneath the DYK and HZS area with northward extension to the shallow depth, which is interpreted as the magma source (Huang *et al*, 2021). Volcanic gas analyses, including helium isotope (Yang *et al*., 1999) and CH_4/ CO_2 gas thermometer, have provided insights into the main magmatic sources or geothermal fluid upwelling area beneath LFG, MT, and DYK (Rae *at al*., 2019; Tong *et al*., 2020). These analyses indicate the presence of multiple reaction sources contributing to the geothermal system.

In the volcanic area, regions with less acidic fluid may be attractive target for geothermal exploration. The TVG geothermal conceptual model has been proposed based on geochemistry studies. Previous studies have identified three main types of hydrothermal fluid in the TVG: acid-sulfate, near-neutral bicarbonate, and acid-sulfate-chloride hot springs (Liu *et al*., 2011). These fluids are associated with different mixing and circulation of magmatic fluid, meteoric water, seawater, or formation water, as well as the interaction with the andesitic or sedimentary rock. However, the most important factor is the water chemistry of the deep reservoir and the volume of the fluids it contains (Dobson *et al*., 2018). The water analyses from Matsao deep well E205, reported a near-neutral pH (~5.6) and a temperature range of 200~300°C. Reports from the alteration mineralogy in the well E208, in the Matsao area, suggested a typical propylitic alteration mineral assemblage (Lan *et al*., 1980). According to the re-examined conceptual model (Rae *et al*., 2019), there may be another up-flow zone surrounding the LHG zone, southwest of CHS. The study also argues that the acid sulphate-chloride fluid may have resulted from mixing of formation water and meteoric water and may not be affected by magmatic fluid. Then, a fourth type of fluid was speculated about in the deep part of southwest CHS (Fig 9). This study identified a possible large-scale andesitic body, where fluids could possibly be neutralized by water-rock interaction. The previous conceptual models provide valuable information for spatially connecting these findings with the results of the geophysical survey. By integrating the collected findings, a comprehensive geothermal conceptual model with 3D subsurface information was developed. This model takes into account the following information:

- Heat source: The possible magma reservoir is located beneath the TVG at a depth of greater than 8 km. The magma reservoir serves as a heat source for the geothermal system. The gases and fluid generated from the magma reservoir upwell predominantly in the CHS and DYK areas, and to a lesser extent in the HZS area. The intruded andesite rock, confirmed by the magnetic model and drilling logs, can act as neutralization agent for the upwelling acid fluids, helping to mitigate their acidity. Additionally, the intrusions contribute to the energy budget within the geothermal system.

- Pathway: The hydrothermal fluid upwelling in the TVG area is influenced by the deep cut structures, which are associated with the tensile tectonic environment in northern Taiwan. The structures depicted in this study align with the speculated pathways for the fluid to migrate toward the surface in a spatial manner. Some volcanic activities observed at the surface are closely correlated with the distinguished fracture systems. These fractures provide conduits for the ascent of volcanic materials and the release of volcanic gases. These upwelling zones are also where the

ISSN 2703-4275

highest temperatures are measured along the northeast trending profile.

- Fluids: Hydrothermal activities, characterized by seismic pattern of inflation, spasmodic burst and a heartbeat-like rhythm, are observed in the CHS and DYK regions. These activities may be caused by the interaction of water and magmatic fluid (Lin *et al*, 2005; Lin, 2017; Pu *et al*., 2020b). The seismic cluster beneath CHS is primarily situated around a relatively high-resistivity core, coupled with an increasing temperature profile, which suggests the presence of an upwelling conduit for geothermal fluids. Another earthquake cluster in the DYK area is situated beneath a low-resistivity anomaly, precisely at the boundary between volcanic rock and sediment layers. The activities of the fluid may be covered by multiple layers of low-resistivity cap rock. There are several zones with resistivity lower than 2 ohm-m that are considered to have a near-neutral chemistry, based on the connection between resistivity and the character of alteration minerals. Part of the geothermal fluid continuously moves upward and reacts with formation water and meteoric water. This interaction occurs as the fluid infiltrates along the topography and follows fracture traces.

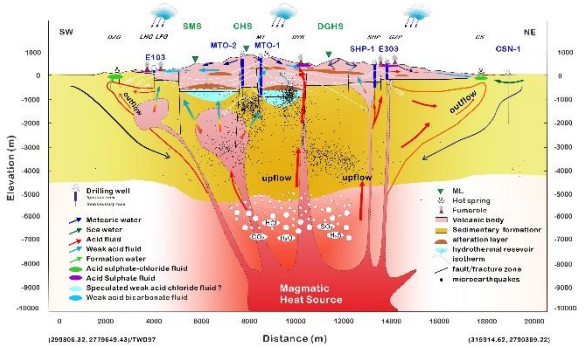

Figure 9: Revised geothermal conceptual model of TVG. The components are based on the new identified geophysical evidence and integrated data from previous studies. Based on downhole testing, MTO-1 has reached a geothermal reservoir with a neutral pH.

3.2 Database

By integrating survey and observation data in the TVG area, comprehensive spatial information covering geological, geophysical, and geochemical aspects has been compiled. Most of the mentioned data are publicly available on the website: https://geotex.geologycloud.tw. To facilitate the integration and analysis of the data, the Leapfrog geothermal software (Seequent Co.) was utilized to build an initial version of the 3D database model. The data incorporated into the model include a geological map, drilling logs, downhole temperature measurements, resistivity models, magnetic models, seismic tomography results, and the epicenters of microearthquakes. The integrated model not only confirms most of the speculations based on evidence but also provides a spatial reference for further exploration and analysis.

CONCLUSION

In this study, fracture channels were interpreted by integrating MT resistivity models, magnetic discontinuity linear features, surface linear features, high-temperature zones, and distributions of micro-seismic activity. These interpretations revealed several deep faults or hydrothermal conduits that connect to the magmatic reservoir and show characteristics detected at the surface. The rebuilt 3D MT model, along with the integration of total magnetic field intensity magnetic susceptibility and gravity density inversion values, indicated the extent of igneous intrusions within the sedimentary rock basement, which corresponded to the recorded andesite bodies in the drilling records.

The geothermal geological conceptual model of the TVG, after incorporating modifications from previous studies, continues to offer new insights. This study supplemented survey items with new data to enhance the spatial understanding of the geothermal conceptual model. Subsequent exploration in the TVG can benefit from the ongoing accumulation of ideas, enabling targeted drilling investigations, such as the fluid chemistry of MT and SMS, and potentially realizing the prospects for geothermal utilization in the Tatun volcanic area at an early stage.

ACKNOWLEDGEMENTS

This work was supported by the Central Geological Survey, Taiwan project B10935: "Prospecting and information integration of Geothermal Geology". The team consists of members from CGS and ITRI who collaborated on this project.

REFERENCES

Chen, W. S., Yang, C. C., Shieh, K. S., Yang, H. C., Chan, Y. C., Liu, J. K., Hsieh, Y. C., (2007). Scanning Laser Mapping (2M×2M DTM) of The Pleistocene Tatun Volcanic Landform. *Bulletin of the Central Geological Survey*, 20, 101-128.

Chu, M. F., Lai, Y. M., Li, Q., Chen, W. S., Song, S. R., Lee, H. Y., (2018). Magmatic pulses of the Tatun Volcano Group, northern Taiwan, revisited: Constraints from zircon U-Pb ages and Hf isotopes. *Journal of Asian Earth Sciences*, 167, 209–217.

Cumming, W., (2016). Resource conceptual models of Volcano-Hosted geothermal reservoirs for exploration well targeting and resource capacity assessment: construction, pitfalls and challenges. *GRC Transactions*, 40, 623–637.

Dobson, P., Gasperikova, E., Spycher, N., Lindsey, N. J., Guo, T. R., Chen, W. S., Liu, C. H., Wang, C. J., Chen, S. N., Flowler, A. P. G., (2018). Conceptual model of the Tatun geothermal system, Taiwan. *Geothermics*, 74, 273–297.

Egbert, G.D. and Kelbert, A., (2012). Computational recipes for electromagnetic inverse problems, *Geophys. J. Int.*, 189, 251–267.

Hsiao, L.-Y.; Lin, K.-A.; Huang, S.-T.; Teng, L.S. Structural Characteristics of the Southern Taiwan-Sinzi Folded Zone. Pet. Geol. Taiwan 1998, 32, 133–153

Huang, H. H., Wu, E. S., Lin, C. H., Ko, J. T., Shih, M. H., & Koulakov, I., (2021). Unveiling Tatun volcanic

plumbing structure induced by post-collisional extension of Taiwan mountain belt. *Sci. Rep*.,11:5286.

Kelbert, A., Meqbel, N., Egbert, G.D., and Tandon, K., (2014). ModEM: A modular system for inversion of electromagnetic geophysical data, *Computers & Geosciences*, 66, 40–53.

Lan, C. Y., Liou, J. G., Seki, Y., (1980). Investigation of drillhole core samples from Tatun geothermal area, Taiwan. In: Proceedings, 3rd International Symposium on Water-Rock Interaction. *Edmonton, Canada*. 183–185.

Lee, C. R., Chiang, D. Y. and Chen, J. H., (1994). Compilation of Geothermal Exploration Data in Taiwan (in Chinese) Research report of Energy Committee, MOEA.

Lee, C. T. and Wang, Y. (1988). Quaternary stress changes in the northern Taiwan and their tectonic implication. Proc. Geol. Soc. China 31 (1), 154–168.

Lin, C. H., Konstantinou, K. I., Liang, W. T. Pu, H. C. Lin, Y. M., You, S. H. and Huang, Y. P., (2005). Preliminary analysis of tectonic earthquakes and volcano-seismic signals recorded at the Tatun volcanic group, northern Taiwan, *Geophysical Research Letters*, Vol. 32, No.10, L10313.

Lin, C. H. (2016). Evidence for a magma reservoir beneath the Taipei metropolis of Taiwan from both S-wave shadows and P-wave delays. Scientific reports, 6(1), 1-9.

Lin, C. H., (2017). Dynamic triggering of drumbeat seismicity at Tatun volcano group in Taiwan, *Geophys. J. Int.*, vol. 210, 354-359.

Lin, C. H., Lai, Y. C., Shih, M. H., Lin, C. J., Ku, J. S. and Huang, Y.C., (2019). A major hydrothermal reservoir underneath the Tatun Volcano Group of Taiwan: Clues from a Dense Linear Geophone Array. *Pure and Applied Geophysics*, https://doi.org/10.1007/s00024-019-02396-w.

Liu, C. M., Song, S. R., Chen, Y. L., Tsao, S., (2011). Characteristics and origins of hot springs in the Tatun volcano group in Northern Taiwan. *Terr. Atmos. Ocean.* Sci. 22, 475–489.

Pu, H. C., Lin, C. H., Hsu, Y. J., Lai, Y. C., Shih, M. H., Murase, M. and Chang, L. C., (2020a). Volcano-hydrothermal inflation revealed through spatial variation in stress field in Tatun Volcano Group, Northern Taiwan. *Journal of Volcanology and Geothermal Research*, 390, 106712. https://doi.org/10.1016/j.jvolgeores.2019.106712.

Pu, H. C., Lin, C. H., Lai, Y. C. Shih, M. H., Chang, L. C., Lee, H. F., Lee, P. T., Hong, G. T., Li, Y. H., Chang, W. Y., Lo, C. H. (2020b). Active Volcanism Revealed from a Seismicity Conduit in the Long-resting Tatun Volcano Group of Northern Taiwan, *Sci Rep*,10, 6153. https://doi.org/10.1038/s41598-020-63270-7.

Rae, A., Reyes, A., Mrozcek, E., and Aunzo, A., (2019). Geothermal resource assessment of the Tatun volcanic group geothermal system-Revision of the conceptual model, Presentation of project results, Taiwan.

Soengkono, S., (2016). Airborne magnetic surveys to investigate high temperature geothermal reservoirs, Advanced in Geothermal Energy Ch. 5, IntechOpen, 37 pp., http://dx.doi.org/10.5772/61651.

Teng, L.S. (1996). Extensional collapse of the northern Taiwan mountain belt. Geology, 24, 949–952.

Teng, L. S., Lee, C. T., Peng, C. H., Chu, J. J. and Chen, W. F. (2001). Origin and geological evolution of the Taipei Basin, northern Taiwan. *West. Pac. Earth Sci.*, 1, 115-142.

Tong, L. T. and Lin, W., (2013). The airborne magnetic survey of onshore and offshore regions in northern Taiwan. *Technical Report of Central Geological Survey*. P188.

Tong, L. T. et al, (2020). Prospecting and information integration of Geothermal Geology. *Technical Report of Central Geological Survey*. P 452.

Song, S. R. and Lo, H. J., (1995). The Source and origin of the volcaniclastics in Linkou Formation of northern Taiwan. *Journal of the Geological Society of China*.38, 3, 287-314.

Tsao, S. J., (1994). Potassium-Argon Age Determination Of Volcanic Rocks From The Tatun Volcano Group. *Bulletin of the Central Geological Survey*, 9, 137-154.

Ussher, G., Harvey, C., Johnstone, R., Anderson, E. (2000). Understanding the resistivities observed in geothermal system, Proceedings World Geothermal Congress 2000, Kyushu-Tohoku, Japan, (2000).

Vavryčuk, V., (2014). Iterative joint inversion for stress and fault orientations from focal mechanisms. *Geophysical Journal International*, 199, 69–77.

Wang, W. H. and Chen, C. H., (1990). The volcanology and fission track age dating of pyroclastic deposits in Tatun Volcano Group. *Acta Geologica Taiwanica* 28, 1–30.

Yang, T. F. and Song, S. R., (1999). 3He/4He ratios of fumaroles and bubbling gases of hot springs in Tatun Volcano Group, North Taiwan. *Nuovo Cimento Della Societa Italiana Di Fisica* C22(3-4), 281–286.

Yeh, C. H., Chan, Y. C., Chang, K. J., Lin, M. L., Hsieh, Y. C., (2014). Derivation of Strike and Dip in Sedimentary Terrain Using 3D Image Interpretation Based on Airborne LiDAR Data. *Terr. Atmos. Ocean.* 25(6), doi: 10.3319/TAO. 2014.07.02.01(TT)

Zellmer, G. F., Rubin, K. H., Miller, C. A., Shellnutt, J. G., Belousov, A. & Belousova, M.,(2015). Resolving discordant U-Th-Ra ages: Constraints on petrogenetic processes of recent effusive eruptions at Tatun Volcano Group, northern Taiwan. *Geological Society Special Publication*. Geological Society of London, 422, 1, 175-188.

ISSN 2703-4275